ADVANCED FUNCTIONAL MATERIALS
www.afm-journal.de

Ordered Honeycomb Structure Surface Generated by Breath Figures for Liquid Reprography

Liping Heng, Jie Li, Muchen Li, Dongliang Tian, Li-Zhen Fan,* Lei Jiang, and Ben Zhong Tang**

In this paper, photoelectric cooperative induced patterned wetting is demonstrated on a hydrophobic ordered polymeric honeycomb structure surface, which is prepared by BF method, then photosensitizing with a dye and hydrophobizing with low-surface-energy materials; finally, photoelectric cooperative induced patterned wetting is achieved on such a hydrophobic honeycomb structure surface. These results indicate that this work is promising for broadening the applications of photoelectric cooperative liquid reprography, which break the limitations of only using inorganic materials and super-hydrophobic materials. It should be of great scientific interest to extend the relevant research from inorganic nanorod, nanopore, and nanotube structures to polymeric honeycomb structures, because polymeric materials can overcome the inherent drawbacks of the inorganic materials owing to their advantages of low specific weight, flexibility, tunable material properties, and wide variety.

1. Introduction

Porous-structured materials, especially highly ordered porous polymeric films have been studied intensively in the past decades. At present, there are several ways to fabricate regularly porous films including templates,[1,2] lithography,[3] emulsions,[4] colloidal crystals,[5,6] and so forth. Among them, the breath figure (BF) process is the simplest method to prepare honeycomb structures, which was firstly reported by François et al. in 1994.[7] After that the formation mechanism of the honeycomb structure has been suggested by François et al.[7] and then revealed by Shimomura and coworkers in detail.[8] This method is more competitive compared to other methods because it is non-polluting, cheaper and faster. In the past ten years, many works have mainly focused on changing polymers and solvents to prepare ordered porous films by the BF process.[9–12] Recently, research focus in this field started to concentrate on fabricating new structures, such as patterned structures and three dimensional structures,[13,14] and developing new function, such as photoelectric conversion,[15] photocatalysis,[16] antireflection,[17] hydrophobicity,[18] high mechanical strength[19,20] and cell adhesion.[21–41] However, their applications, particularly in the liquid reprography aspects, have not yet drawn the scientific attention.

Stimuli-responsive surface wettability has been intensively studied under external stimulus such as thermal treatment,[24] pH,[25,26] light irradiation,[27–29] electric fields,[30,31] and solvent treatment.[32,33] Specially, the cooperation of two different stimuli seems to be a trend for more effective surface wetting tunability.[34–37] Among them, the photoelectric cooperation stimulus is a more-effective way for regulating surface wettability. Recently, our group achieved the patterned wettability transition from the Cassie[38] to the Wenzel state[39] on superhydrophobic surfaces such as aligned-ZnO-nanorod array surface,[40] aligned-nanopore array surface of TiO_2 -coated nanoporous AAO film[41] and CdS quantum dots sensitized TiO_2 nanotubes[42] by photoelectric cooperative wetting process, which had been used for liquid reprography. However, all of these surfaces reported above based on inorganic materials are prone to damage due to their low mechanical strength and high frangibility, so they could not sustain repeated printing. Meanwhile, because of the limited categories of the inorganic materials, their practical application was limited. In addition, all of these surfaces reported above are superhydrophobic surfaces, while the practical applications of superhydrophobic surfaces are still not universal because there are many problems needed to be solved. Firstly, it is difficult to prepare a large area of superhydrophobic surfaces because of the harsh preparation conditions. Secondly, superhydrophobic surfaces are not stable and robust

Prof. L. P. Heng, Prof. D. L. Tian, Prof. L. Jiang
School of Chemistry and Environment
Beihang University
Beijing 100191, China
E-mail: henglp@iccas.ac.cn
Prof. L. P. Heng, Prof. L. Jiang
Beijing National Laboratory for Molecular Sciences (BNLMS)
Key Laboratory of Organic Solids
Institute of Chemistry Chinese Academy of Sciences
Beijing 100190, China
Dr. J. Li, Prof. B. Z. Tang
Institute for Advanced Study
Institute of Molecular Functional Materials and Division of Biomedical Engineering
the Hong Kong University of Science & Technology
Clear Water Bay, Kowloon
Hong Kong, China
E-mail: tangbenz@ust.hk
Dr. M. C. Li, Prof. L.-Z. Fan
Institute of Advanced Materials and Technology
University of Science and Technology Beijing
Beijing 100083, China
E-mail: fanlizhen@ustb.edu.cn

DOI: 10.1002/adfm.201401342

because micro-structures of the superhydrophobic films were easily damaged or scraped by external forces in the long-term operation process, which could result in a gradual loss of superhydrophobicity. As a result, it is difficult to apply liquid reprography on such an inorganic superhydrophobic surface. Hence, a robust film with good flexibility and excellent stability of hydrophobicity for photoelectric cooperative liquid reprography towards practical applications is still a challenge. The geometry of the honeycomb structure is ordered-pore array which is similar to AAO membranes.[41] Such a structure is expected to display excellent liquid reprography behavior. It should be interesting to extend the relevant research from inorganic nanorod, nanopore and nanotube structures to polymeric honeycomb structures, because polymeric materials can overcome the inherent drawbacks of the inorganic materials owing to their advantages of low specific weight, flexibility, tunable material properties and wide variety. To our best knowledge, the development of honeycomb structure surface by using polymeric materials for liquid reprography is still a challenge for modern science.

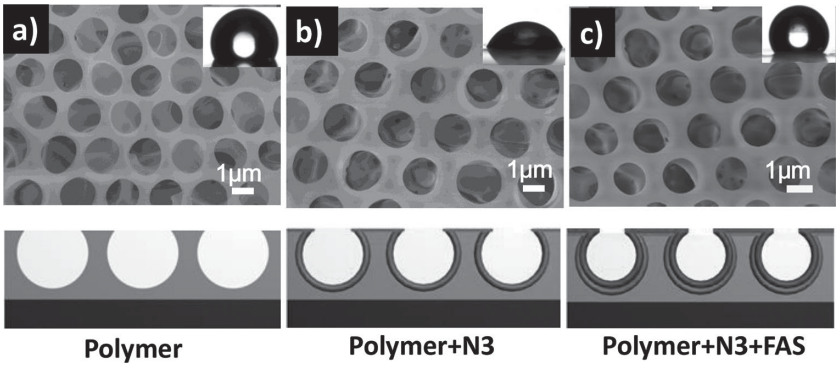

Figure 1. SEM images, water CA photographs, and schematic diagrams of the as-prepared honeycomb structure film. Top view SEM image (top) and schematic diagrams (bottom) of the as-prepared a) polymer honeycomb structure, b) N3 dye coated polymer honeycomb structure, and c) polymer honeycomb structure sensitized by N3 dye and modified with FAS. Inset photographs show the corresponding CAs on respective surface are 120.3 ± 5.1°, 69.7 ± 2.8°, 122.5 ± 3.3°.

Here, we displayed photoelectric cooperative induced patterned wetting on a hydrophobic ordered polymeric honeycomb structure surface. The hydrophobic honeycomb structure surface was prepared by BF method, then photosensitizing with a dye and hydrophobizing with low-surface-energy materials; finally, photoelectric cooperative induced patterned wetting was achieved on such a hydrophobic honeycomb structure surface. The patterned wetting process on this structure was easily controlled by the parallel structure of the adjacent pores. This work will promote the practical applications of photoelectric cooperative liquid reprography, which break the limitations of only using inorganic materials and super-hydrophobic materials.

2. Results and Discussion

2.1. Fabrication of the Hydrophobic Honeycomb Structure Surface

The mechanism of honeycomb formation has been described by several authors[8–12] and will be only briefly outlined here. When the water-immiscible organic solvent starts to evaporate, the solution surface temperature decreases. Water from the atmosphere starts to condense. Because the condensation takes place on an unstructured liquid surface, the water droplets have a narrow size distribution. With ongoing evaporation of the organic solvent, these water droplets can grow until the solution becomes too viscous. The droplets of the condensed water self-assemble into a hexagonally ordered array at the air/solution interface. After the evaporation of solvent and water droplets, the well-ordered honeycomb structure is left on the film surface. The detail synthesis and characterization information of polymer 1 (P1) used in experiments is shown in Chart S1 (Supporting Information). The UV–Vis spectra of P1 in THF solution show that its absorption peak appears in the region of around 340 nm (Figure S1a, Supporting Information). The UV–Vis spectra of P1 solid film show that its absorption peak appears in the region of around 300–400 nm (Figure S1b, Supporting Information). These curves illustrated that the solid state absorption peak red shifts comparing with P1 solution, the light can be hardly absorbed by the p1 solid film when the wavelength is larger than 450 nm. Photoluminescence (PL) spectra of P1 in THF/hexane mixtures with different hexane volume fractions are shown in the Figure S2 (Supporting Information), and it is found that the PL intensity is enhanced with increase of the non-solvent hexane volume fraction. That is to say, this molecule has the aggregation-induced emission (AIE) property.[43,44] The AIE feature of this polymer will benefit the study of photoelectric cooperative wetting mechanism, which will be discussed in detail as follows.

Figure 1 shows the scanning electron microscopy (SEM) images, water-contact angle (CA) photographs, and schematic diagrams of the as-prepared porous structure film. Figure 1a and Figure 1b are the top-view SEM images before and after the honeycomb structure film were sensitized with *cis* -bis(4,4′-dicarboxy-2,2′-bipyridine) dithiocyanato ruthenium(II) (N3 dye), respectively. Figure 1c is the SEM image after the film was modified by heptadecafl uorodecyl-trimethoxysilane (FAS) (Figure S3, Supporting Information), which can improve the surface hydrophobicity, and protect their morphologies from being damaged. In fact, the pore inner surface can be modified by N3 dye and FAS. The honeycomb-patterned films were sensitized by a solution (0.5 mmol L^{-1}) of N3 dye in dry ethanol by dip coating method, then treated with the vapor of heptadecafluorodecyl-trimethoxysilane (FAS) for 3 h. Ethanol CA on the porous films is about 0°(shown in the Figure S4, Supporting Information). So N3 ethanol solution can enter into the pores due to the capillary effect on this superhydrophilic film. The solution can completely fill the pore and the pore inner surface can be modified by N3 dye. Then the pores were treated with the vapor of heptadecafluorodecyl-trimethoxysilane (FAS) which can enter the pore inner surface, forming the structure of Figure 1c. The pore diameter is about 1.5 μm, while the

average wall between two pores increased from (0.5 ± 0.1) to (0.8 ± 0.2) and (0.8 ± 0.2) μm, respectively. Inset photographs show the corresponding CAs on respective surface are 120.3 ± 5.1°, 69.7 ± 2.8°, 122.5 ± 3.3°, indicating that the N3 sensitizer decreased the CA, while FAS modification can increased the hydrophobicity of the surface. As a result, the prepared honeycomb structure surface was tuned to be a hydrophobic surface with a CA of 122.5 ± 3.3° (Figure 1c). More importantly, the honeycomb structure film was kept well during the printing process as shown in Figure S5 (Supporting Information), demonstrating the robustness and reliability offered by organic polymeric materials. Meanwhile the side-view SEM images indicate that the pores are grown almost perpendicularly onto the substrate with a thickness of about 4 μm, and the adjacent pores have been separated each other by the wall.

2.2. Wettability Transition on the Honeycomb Structure Surface Induced by Photoelectric Cooperation Stimulus

Wettability changes on the honeycomb structure surface induced by electric fields and photoelectric cooperation stimulus were studied systematically. **Figure 2**a–c show the electrowetting phenomenon investigated on the honeycomb structure surface. We can see that the honeycomb structure surface had a CA of about 120° (Figure 2a) at the initial stage. When a voltage of 24.9 V was applied, the CA began to decrease and finally reached <5° at 33.6 V (Figure 2b), but the CA did not change after the voltage was turned off (Figure 2c). That is to say, the electrowetting happened when the applied voltage ranged from 24.9 V to 33.6 V. Analogically, photoelectric cooperative wetting was examined, as illustrated in Figure 2d–f.

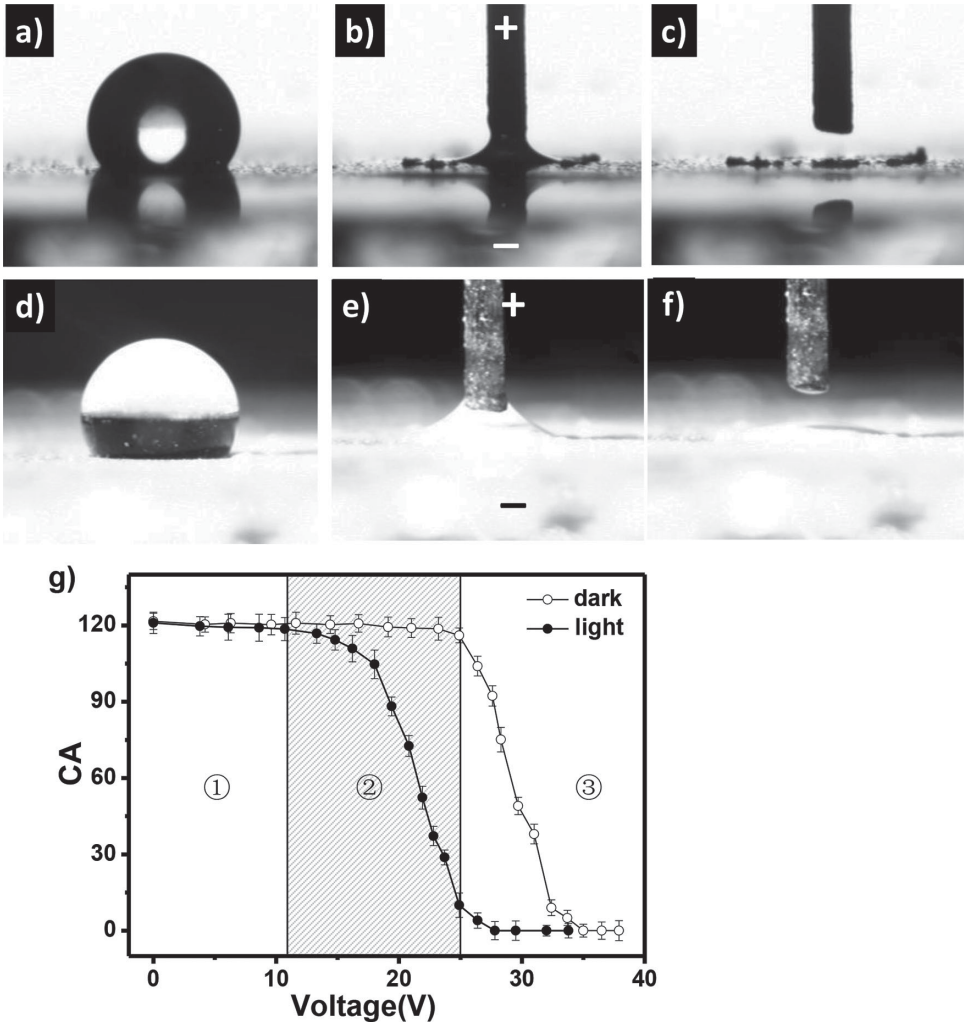

Figure 2. Electrowetting and photoelectric cooperative wetting on the honeycomb structure film surface. a) With no voltage applied, the CA is around 120°. b) The CA decreases finally reaches <5° at 33.6 V. c) After the voltage is turned off, the CA does not change. d) With light illumination, the CA is around 120° at 0 V. e) With light illumination, the CA decreases and finally reaches <5° at 26.4 V. f) After the light and the voltage are turned off, the CA remains the same. g) The CA as a function of the applied voltage is measured with (●) and without (○) light illumination. The applied voltage can be divided into three regions: in region ①, electrowetting cannot occur, even with light illumination; in region ②, electrowetting takes place with light illumination; in region ③, electrowetting also happens without light illumination. Region ② is considered to be the suitable work-around for photoelectric cooperative wetting. The symbols "+" and "–" represent the anode and cathode of the electrical source, respectively.

When white light with an intensity of about 240 mW cm^{-2} illuminated the surface, and a voltage of 10.8 V was applied, the CA began to decrease and finally reached <5° at 26.4 V. (Figure 2e). Similarly, the CA remained almost the same, even after the light and the voltage were turned off (Figure 2f). Here the photoelectric cooperative wetting appeared as the applied voltage ranged from 10.8 V to 26.4 V. Eventually, a remarkable wettability transition was realized with a CA change as large as 120°. Based on the CA versus voltage curve of electrowetting as shown in Figure 2g, the threshold voltage was about 24.9 V without light, while it was about 10.8 V with light. It is evident that the CA finally reached <5° both without and with light illumination, while the former situation needed a higher voltage for electrowetting. According to the conditions of electrowetting, the applied voltage can be divided into three regions. In region ①, electrowetting cannot occur because the applied voltage does not reach the threshold voltage; in region ②, electrowetting takes place under light illumination because the light illumination reduces the threshold voltage; in region ③, electrowetting also happens even without light illumination, owing to the applied voltage exceeding the threshold voltage. Thus, region ② is considered to be the suitable workaround for photoelectric cooperative wetting. It should be noted that inorganic materials have the contact angle saturation during the photoelectric collaborative wetting testing process,[40–42] but the polymeric materials have no this phenomenon, since the film will be broken when the applied voltage is above 26.4 V. This situation is also found in our other studies. Considering the CA change range and the film stability during photoelectric cooperative wetting, a voltage of 21 V was chosen for the following study. These results strongly demonstrate that photoelectric cooperative induced wetting can be realized on the honeycomb structure surface fabricated by using organic polymeric materials.

2.3. Liquid Reprography on the Honeycomb Structure Surface

In order to examine the possibility of liquid reprography induced by patterned-light illumination on the honeycomb structure surface, a detailed process was given **Figure 3**, in which the testing method was similar to that described in the literature.[40–42] When the commercial water-soluble ink was added onto the honeycomb structure surface below the threshold voltage, air was trapped in the pores[45] (Figure 3a), which is attributed to the transitional state between Wenzel's and Cassie's state of the hydrophobic surface (this transitional state was confirmed by calculation, shown in Figure S6, Supporting Information).[46] With the patterned light (i.e., "▲") illuminating the honeycomb structure surface through a photo mask, the wettability of the patterned-site transferred from the transitional state to the Wenzel state (Figure 3b),[39] and thus the ink entered into the pores. After the light and the voltage were turned off, the ink pattern "▲" was left with the removal of redundant ink (Figure 3c). Finally, the ink pattern was easily transferred from the honeycomb structure surface onto hydrophilic printing paper, and the desired reprographic image, "▲", was successfully obtained (Figure 3d). Similarly, other

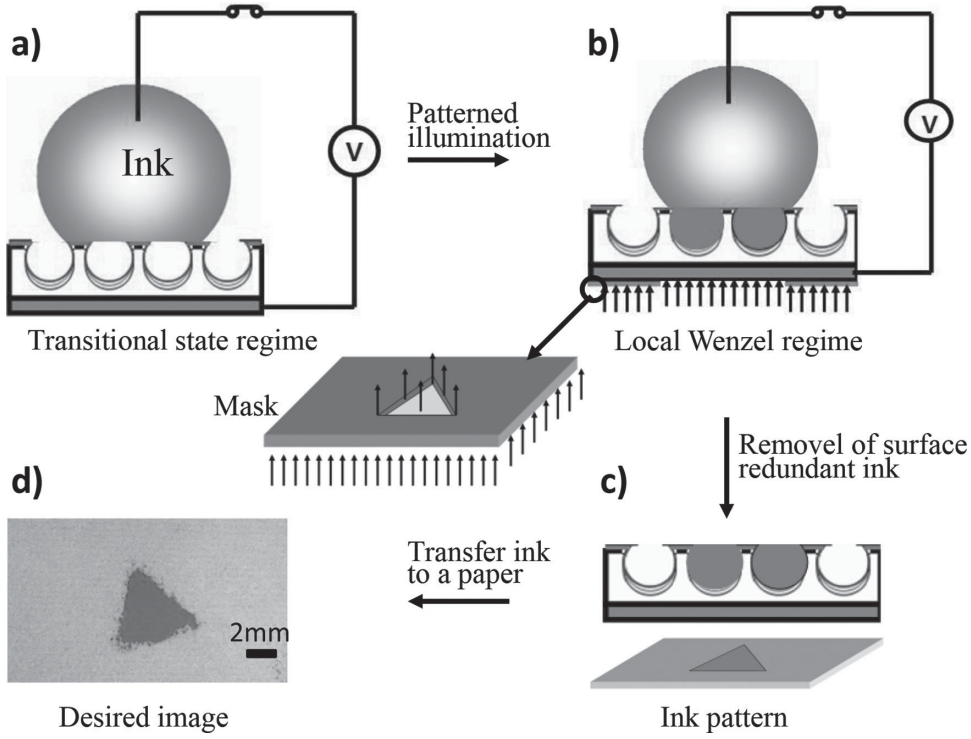

Figure 3. Schematic diagrams of the liquid reprography process. a) Surface wettability behaves hydrophobic transitional state below the electrowetting threshold voltage. b) Surface wettability locally transits from transitional state to Wenzel state under the patterned light "▲" illuminating to the porous structure film below the electrowetting threshold voltage. c) After the light and the voltage are turned off, ink pattern "▲" is left with the removal of redundant ink. d) When the ink pattern is transferred onto a printing paper, the desired image "▲" is obtained.

reprographic images can also be obtained. During the liquid-reprography process, when the applied voltage exceeds the threshold voltage, photoelectric cooperative wetting occurs, the surface wettability of the porous film changes from hydrophobic to hydrophilic at the patterned illumination site. After the light and the voltage are turned off, the hydrophilicity of the region remains almost the same. Based on this character, ink can enter into the pores due to the capillary effect in this hydrophilic region. The other region is still the original hydrophobic state due to the low-surface-energy compound modification. Thus the residual ink on the hydrophobic region can be removed by the filter paper carefully. Here, we can see the picture marginal was not clear because the reprographic resolution is not high. In fact, the resolution of liquid reprography is related to the pore diameter. The smaller the pore diameter is, the higher the resolution is. In this work, the pore diameter is about 1.5 μm. Thus, resolution of liquid reprography is not so high.

2.4. Mechanism of Photoelectric Cooperative Liquid Reprography on the Honeycomb Structure Surface

To understand the mechanism of this photoelectric cooperative liquid reprography on the honeycomb structure surface, the photoconductivity property and the special surface structure of the honeycomb structure should be carefully examined. Here, the N3-dye-sensitized organic honeycomb structure film, as a composite photoconductor layer, shows good photoconduction in the visible region. The UV–vis diffuse-reflectance spectra in **Figure 4**a show that the N3-dye- sensitized organic honeycomb structure film presented much-weaker light reflection at around 400–700 nm than that of before sensitization, thus allowed maximum harvesting of light in the UV–vis region. The photocurrent action spectrum in Figure 4b shows that the N3-dye-sensitized- organic honeycomb structure film had a broad photoelectric response over almost the whole region around 450–700 nm, indicating that the N3 dye could strongly sensitize the organic honeycomb structure film. As shown in **Figure 5**a,b, the electrochemical impedance decreased greatly under the illumination, illustrating that this polymer composite system has a good photoconductivity property. The Nyquist diagrams of the impedance spectra obtained in the dark and under illumination for the N3-dye-sensitized- honeycomb structure film in Figure 5c showed that the film had a high electrical resistance in the dark, acting as a dielectric layer, while it presented a lower electrical resistance under illumination as a conductive layer. And the bode diagrams of the electrochemical impedance spectra obtained in the dark and under light illumination for the N3-dye-sensitized-polymer honeycomb structure film as shown in Figure 5d measured under the illumination of one sun at open-circuit potential. From the medium-frequency semicircle in the bode plots, it can be seen that the low frequency peak of film under illumination is shifted to high frequency compared with that in dark, verifying that the interfacial charge recombination between the photo-injected electron and electrolyte materials was encumbered.

These results indicate that the N3 dye strongly sensitized the honeycomb structure film due to the efficient electron transfer from the polymer to the excited state of the N3 dye, as illustrated

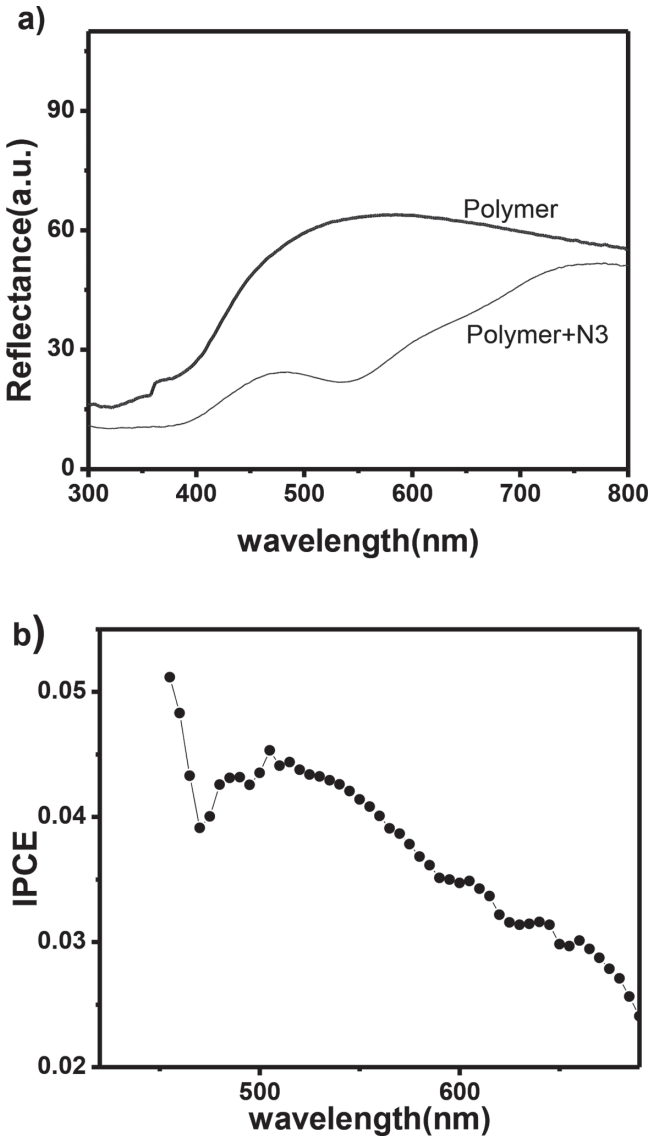

Figure 4. The photoelectric-properties characterization of the N3-dye-sensitized- polymer films. a) UV–vis diffuse-reflectance spectra of polymer honeycomb film and N3-dyesensitized- polymer honeycomb films. b) Photocurrent action spectrum of the N3-dye-sensitized-polymer honeycomb film.

in detail in **Figure 6**a. The lowest unoccupied molecular orbital (LUMO) energy levels of P1 and the N3 dye are –2.7 eV and –3.6 eV (Figure S7, Supporting Information), respectively. The highest occupied molecular orbital (LOMO) energy levels of P1 and the N3 dye are –5.6 eV and –5.7 eV (Figure S7, Supporting Information), respectively. N3 molecule is easily excited by white light because it has a broad absorption in the visible light region (shown in Figure S8, Supporting Information). Excited-state N3 is both a very good electron acceptor and an excellent electron donor material. Here N3 molecule is an electron acceptor material according to their energy levels. So the efficient electron transfer from the polymer to the excited state of the N3 dye occurred when the film was irradiated by the white light. Efficient photoinduced electron transfer is a prerequisite

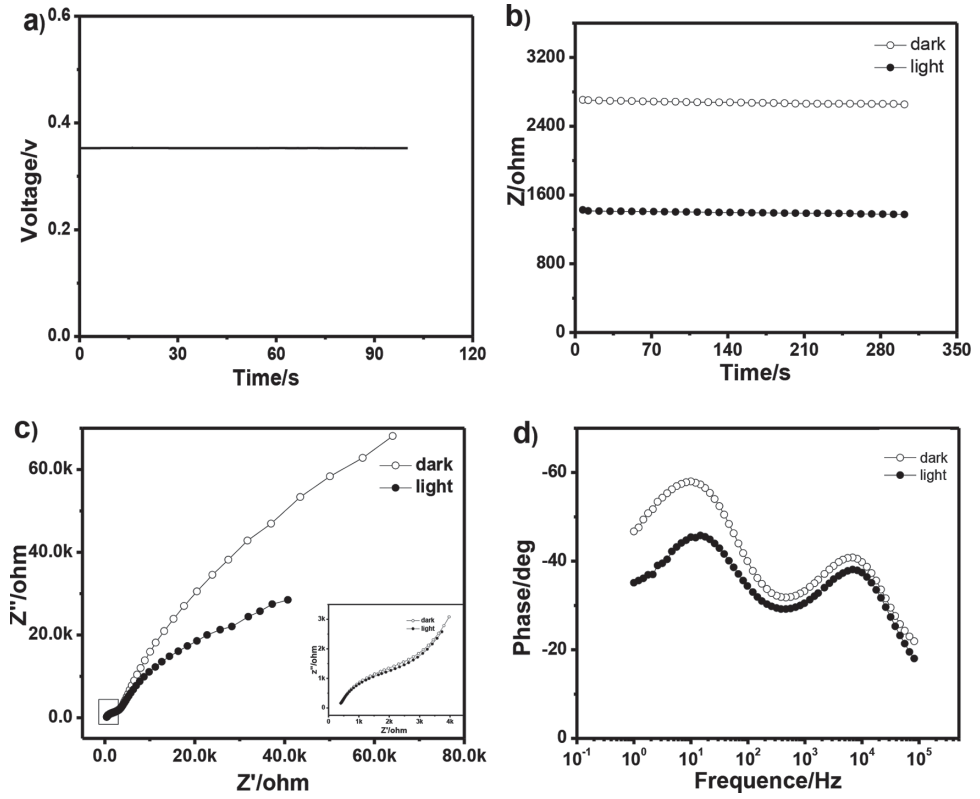

Figure 5. a) Variations of the open circuit voltage with the time, b) Variations of the electrochemical impedance with the time, c) Nyquist and d) Bode diagrams of the electrochemical impedance spectra obtained in the dark and under light illumination for the N3-dye-sensitized-polymer honeycomb films. The inset shows the corresponding enlarged drawing. The spectra were measured under the illumination of one sun at open-circuit potential.

for achieving efficient liquid reprography in organic composite systems. Here, both the top and the inner surface N3 modification play a key role for the liquid reprography, because the photoelectric cooperative wetting effects is related to the total amount of dye. If we only modified the top surface, the total amount of dye is small which can make the threshold voltage large and the work-around small. The photoelectric cooperative wetting effects are affected and difficult to achieve the liquid reprography. One concern that might arise is whether the photoinduced electron transfer occurs between the dye and polymer molecules. We also test the efficiency of photoinduced electron transfer through photoluminescence (PL) measurements. As shown in Figure 6b, although the FL intensity of polymer in solution is genuinely weak P1 is highly emissive in its solid state, demonstrating its AIE property. But in the N3 dye sensitized- honeycomb structure film, direct contact of the dye layer with the polymer layer led to a dramatically reduced PL intensity from polymer due to the efficient photo-induced electron transfer in the interpenetrating donor/acceptor network by inter-diffusion of dye into the pores of polymer matrix. Consequently, the effective thickness of the dielectric layer decreases, as described by Equation 1,[47] the threshold voltage drops, and then electrowetting happens.

$$\cos\theta_V = \cos\theta_0 + \frac{\varepsilon_0\varepsilon_1}{2d\gamma_{LV}}(V - V_T)^2 \quad (1)$$

where θ_0 is the initial CA with no voltage applied, θ_V is the CA at a voltage V, ε_0 is the permittivity of vacuum, ε_1 is the permittivity of the dielectric layer, d is the thickness of the dielectric layer, γ_{LV} is the surface tension of the liquid–vapor interface, and V_T is the voltage that needs to compensate the influence of the trapped charges.

Compared to the smooth surface with the CA of (88.2 ± 2.3)° (advancing angle $\theta_{a,0}$ = (105.3 ± 1.8)°), the pore surface has a higher CA of (122.8 ± 2.6)° (advancing angle θ_a = (138.7 ± 1.2)°), suggesting that the pore surface is the transitional state between Wenzel's and Cassie's state (see Figure S6 in Supporting Information). To further thoroughly understand the mechanism of the patterned wettability transition, we model the wetting of the ordered honeycomb structure surface in **Figure 7**, on the assumption that the pores were arranged approximately in a regular, hexagonal array with an average pore diameter of 1.5 ± 0.3 μm and a spacing of 0.8 ± 0.2 μm (based on Figure 1c). From Figure 7, it is clear that electrowetting occurs only at the illumination site. The reason why the pores are effective at preventing spontaneous transitions from the transitional state to the Wenzel state is due to the advancing angle, $\theta_{a,0}$, that the liquid has to exceed in order to wet the bottom of each pore. Accordingly, the liquid will stay on top of the pores and remain in the transitional state between Wenzel's and Cassie's state unless an external pressure is applied to overcome the hydrostatic pressure, ΔP, which must be exceeded before water will intrude into the pores. ΔP is given as:[48]

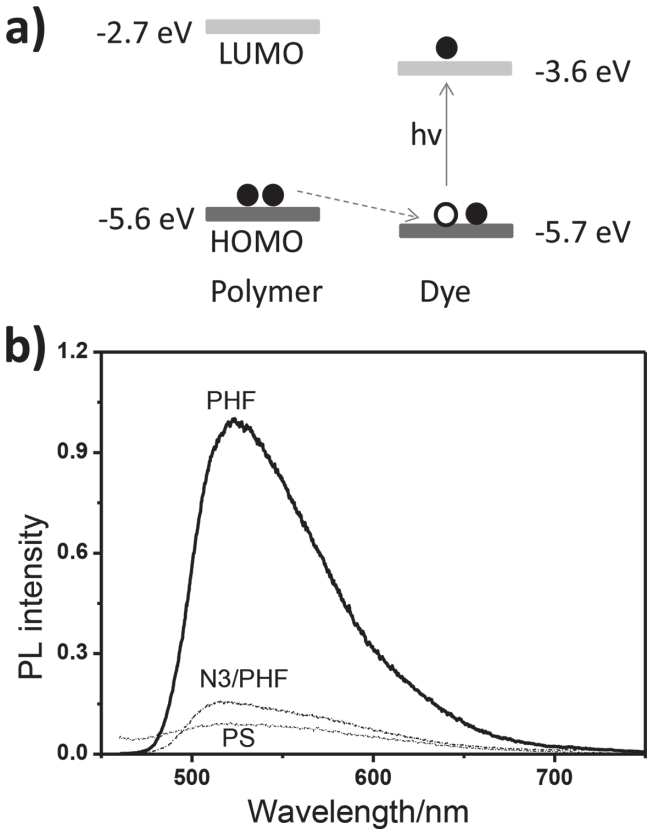

Figure 6. a) Schematic energy level diagram of the N3-dye-sensitized-polymer honeycomb structure film and photoexcited electron transfer process, b) PL spectra of polymer honeycomb film (PHF), polymer honeycomb film coated with N3 dye(N3/PHF), and polymer solution (PS). Excitation: 450 nm.

$$\Delta P = -l\gamma_{LV}(\cos\theta_A)/A \quad (2)$$

In Equation 2, l is the circumference of a pore, A is the cross-sectional area of a pore and θ_A is the advancing angle of liquid on the surface. Equation 2 predicts the hydrostatic pressure to be 9.82×10^4 Pa, which is a considerable wetting-energy barrier at atmospheric pressure and must be overcome if the liquid is to intrude into the pores. For the illumination site, photoelectric cooperative wetting induces the CA to decrease and causes an electrocapillary pressure, ECP, which is given by:[49]

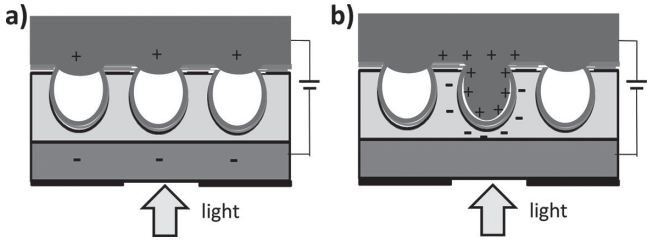

Figure 7. Schematic diagrams of the wetting model of the as-prepared honeycomb structure film. a) the initial state schematic diagrams. It shows that wetting does not occur when $P < \Delta P$; and b) are the final liquid wetting state schematic diagrams of the illumination site. It clearly shows that electrowetting occurs only at the illumination site when $P > \Delta P$.

$$\mathrm{ECP} = \frac{l\Delta\gamma}{A} = \frac{1}{2}\frac{l}{A}\frac{\varepsilon_0\varepsilon_1}{d}(V - V_T)^2 \quad (3)$$

The ECP can promote the influx of the liquid into the pores, as long as the condition ECP ≥ ΔP is satisfied. Calculated by Equation 3, the ECP was 1.1×10^5 Pa in this study, which was enough to overcome the hydrostatic pressure, ΔP. Meanwhile, the liquid could not spread to the unilluminated sites, on account of the solid-wall blocking. Clearly, the clear ink pattern on the aligned-pore array structure could be easily controlled because only the condition of $\Delta P \leq$ ECP was needed, showing the excellent controllability.[50]

3. Conclusions

In conclusion, we have demonstrated the photoelectric cooperative induced patterned wetting process on the hydrophobic organic polymer honeycomb structure film surface. The ordered photoconductive pore array provides a wetting condition for the patterned wettability transition, and micro-scale liquid can be controlled by designing the nanostructures of the surface and controlling the ECP. Liquid reprography has been achieved through the patterned wetting process on the hydrophobic organic honeycomb structure film surface, which is a novel concept for the organic honeycomb structure system, represents new progress in liquid reprography and is promising for broadening the application of photoelectric cooperative liquid reprography. This result is of great scientific interest to extend the relevant research from inorganic materials to polymer materials.

4. Experimental Section

Preparation of the Hydrophobic Honeycomb Structure Surfaces: P1 used in this experiment with a molecular weight of about 23 400 was synthesized according to the literature. The detail synthesis and characterization information was in Chart S1. P1 solutions with different concentration were prepared by dissolving appropriate amounts of polymer in chloroform. Water was purified using a Milli-Q purification system (Millipore Corp., Bedford, MA) to give a resistivity of 18 MW cm^{-1}. A solution of polymer 1 in chloroform (100 μL, 2 mg mL^{-1}) was cast on cleaned ITO substrates at room temperature (24 ± 1 °C) under a humid atmosphere with relative humidity of about 85%, and honeycomb-patterned films were obtained. Subsequently, the honeycomb-patterned films were sensitized by a solution (0.5 mmol L^{-1}) of N3 dye in dry ethanol and then dried at 60 °C for 1 h, then treated with the vapor of heptadecafluorodecyl-trimethoxysilane (FAS) for 3 h. The composite honeycomb-patterned films dielectric layer for the photoelectric cooperative induced wetting process was then obtained, with a thickness of 4–5 μm. More importantly, a smooth polymer layer was also formed at the air/ITO interface when the polymer solution was coated onto the ITO (Figure S5c, Supporting Information). FAS coated onto the N3-sensitized honeycomb-patterned films were used to prevent electrolysis to damage N3 molecule during the electrowetting measurements.

Instruments and Characterization: SEM images were obtained using a JEOL JSM-6700F SEM at 3.0 kV. The CAs were measured using a Dataphysics OCA20 CA system at ambient temperature. A 2 μL water droplet was used in all of the water-CA measurements. At least five different positions were measured and averaged to get a reliable value, using the same sample. A solar simulator (CMH-250, Aodite

Photoelectronic Technology Ltd., Beijing) was used as the light source. The applied voltage in the electrowetting measurements was supplied by a dc power source; the corresponding voltages were obtained directly without time steps to achieve more-exact data in the experiment. UV–Vis spectra were obtianed using a Hitachi U-3010 UV–Vis spectrometer, and fluorescence spectra were recorded on a Hitachi F-4500 fluorescence spectrophotometer. The electrochemical impedance measurements were carried out on a Zahner IM6eX impedance analyzer (Germany) under illumination of 100 mW cm^{-2} and open-circuit conditions. The action spectra of the monochromatic incident photo-to-current conversion eciency (IPCE) for solar cells were collected using a commercial setup (PV-25 DYE, JASCO). A 300 W Xenon lamp was employed as light source for generation of a monochromatic beam. The electrochemical cyclic voltammetry (CV) was conducted on a CHI650D electrochemical workstation with glassy carbon, platinum wire, and Ag/Ag+ electrode as working electrode, counter electrode and reference electrode respectively, in a 0.1 M tetrabutylammonium hexauorophosphate (Bu4NPF6) acetonitrile solution.

Supporting Information

Supporting Information is available from the Wiley Online Library or from the author.

Acknowledgements

This work was supported by the National Research Fund for Fundamental Key Projects (2013CB834705, 2010CB934700, 2011CB935703, 2013CB934001), and the National Natural Science Foundation of China (Grant No. 21207076, 51172024, and 51372022).

Received: April 26, 2014
Revised: June 12, 2014
Published online: August 22, 2014

[1] A. Joy, S. Uppili, M. R. Netherton, J. R. Scheffer, V. Ramamurthy, *J. Am. Chem. Soc.* **2000**, *122*, 728.
[2] Q. B. Meng, C. H. Fu, Y. Einaga, Z. Z. Gu, A. Fujishima, O. Sato, *Chem. Mater.* **2002**, *14*, 83.
[3] P. T. Tanev, M. Chibwe, T. J. Pinnavaia, *Nature* **1994**, *168*, 321.
[4] A. Imhof, D. J. Pine, *Nature* **1997**, *389*, 948.
[5] J. A. Rogers, K. E. Paul, R. J. Jackmann, G. M. Whitesides, *Appl. Phys. Lett.* **1997**, *702*, 658.
[6] Y. Li, W. Cai, G. Duan, *Chem. Mater.* **2008**, *60*, 215.
[7] G. Widawski, M. Rawiso, B. Francois, *Nature* **1994**, *369*, 387.
[8] N. Maruyama, O. Karthaus, K. Ijiro, M. Shimomura, T. Koito, S. Nishimura, T. Sawadaishi, N. Nishi, S. Tokura, *Supramol. Sci.* **1998**, *5*, 331.
[9] B. De Boer, P. F. Van Hutten, C. Melzer, V. V. Krasnikov, G. Hadziioannou, *Polymer* **2001**, *42*, 9097.
[10] L. V. Govor, I. A. Bashmakov, R. Kiebooms, V. Dyakonov, J. Parisi, *Adv. Mater.* **2001**, *13*, 588.
[11] C. X. Cheng, Y. Tian, Y. Q. Shi, R. P. Tang, F. Xi, *Langmuir* **2005**, *21*, 6576.
[12] T. Nishikawa, J. Nishida, R. Ookura, S. I. Nishimura, V. Scheumann, M. Zizlsperger, R. Lawall, W. Knoll, M. Shimomura, *Langmuir* **2000**, *16*, 1337.
[13] J. H. Kim, M. Seo, S. Y. Kim, *Adv. Mater.* **2009**, *21*, 4130.
[14] L. A. Connal, R. Vestberg, C. J. Hawker, G. G. Qiao, *Adv. Funct. Mater.* **2008**, *18*, 3706.
[15] L. P. Heng, J. Zhai, Y. Zhao, J. J. Xu, X. L. Sheng, L. Jiang, *ChemPhysChem* **2006**, *7*, 2520.
[16] K. Kon, C. N. Brauer, K. Hidaka, H. G. Lohmannsroben, O. Karthaus, *Langmuir* **2010**, *26*, 12173.
[17] M. S. Park, J. K. Kim, *Langmuir* **2005**, *21*, 11404.
[18] H. Yabu, M. Takebayashi, M. Tanaka, M. Shimomura, *Langmuir* **2005**, *21*, 3235.
[19] X. Xu, L. P. Heng, X. J. Zhao, J. Ma, L. Lin, L. Jiang, *J. Mater. Chem.* **2012**, *22*, 10883.
[20] L. P. Heng, B. Wang, M. C. Li, Y. Q. Zhang, L. Jiang, *Materials* **2013**, *6*, 460.
[21] T. Nishikawa, J. Nishida, R. Ookura, S. I. Nishimura, S. Wada, T. Karino, M. Shimomura, *Mater. Sci. Eng. C* **1999**, *10*, 141.
[22] M. Tanaka, *Biochim. Biophys. Acta* **2011**, *1810*, 251.
[23] T. Nishikawa, M. Nonomura, K. Arai, J. Hayashi, T. Sawadaishi, Y. Nishiura, M. Hara, M. Shimomura, *Langmuir* **2003**, *19*, 6193.
[24] G. D. Crevoisier, P. Fabre, J. M. Corpart, L. Leibler, *Science* **1999**, *285*, 1246.
[25] X. Yu, Z. Q. Wang, Y. G. Jiang, F. Shi, X. Zhang, *Adv. Mater.* **2005**, *17*, 1289.
[26] F. Xia, H. Ge, Y. Hou, T. L. Sun, L. Chen, G. Z. Zhang, L. Jiang, *Adv. Mater.* **2007**, *19*, 2520.
[27] R. Wang, K. Hashimoto, A. Fujishima, M. Chikuni, E. Kojima, A. Kitamura, M. Shimohigoshi, T. Watanabe, *Nature* **1997**, *388*, 431.
[28] X. J. Feng, J. Zhai, L. Jiang, *Angew. Chem. Int. Ed.* **2005**, *44*, 5115.
[29] H. S. Lim, J. T. Han, D. Kwak, M. H. Jin, K. Cho, *J. Am. Chem. Soc.* **2006**, *128*, 14458.
[30] M. W. J. Prins, W. J. J. Welters, J. W. Weekamp, *Science* **2001**, *291*, 277.
[31] Z. K. Wang, L. J. Ci, L. Chen, S. Nayak, P. M. Ajayan, N. Koratkar, *Nano Lett.* **2007**, *7*, 697.
[32] S. Minko, M. Muller, M. Motornov, M. Nitschke, K. Grundke, M. Stamm, *J. Am. Chem. Soc.* **2003**, *125*, 3896.
[33] L. P. Heng, Y. Q. Dong, J. Zhai, B. Z. Tang, L. Jiang, *Langmuir* **2008**, *24*, 2157
[34] F. Xia, L. Feng, S. T. Wang, T. L. Sun, W. L. Song, W. H. Jiang, L. Jiang, *Adv. Mater.* **2006**, *18*, 432.
[35] Y. Guo, F. Xia, L. Xu, J. Li, W. S. Yang, L. Jiang, *Langmuir* **2010**, *26*, 1024
[36] W. Sun, S. X. You, L. M. Wu, *J. Mater. Chem. A* **2013**, *1*, 3146.
[37] P. Y. Chiou, H. Moon, H. Toshiyoshi, C. J. Kim, M. C. Wu, *Sens. Actuators A* **2003**, *104*, 222.
[38] A. B. D. Cassie, S. Baxter, *Trans. Faraday Soc.* **1944**, *40*, 546.
[39] R. N. Wenzel, *Ind. Eng. Chem.* **1936**, *28*, 988.
[40] D. L. Tian, Q. W. Chen, F. Q. Nie, J. J. Xu, Y. L. Song, L. Jiang, *Adv. Mater.* **2009**, *21*, 3744.
[41] D. L. Tian, J. Zhai, Y. L. Song, L. Jiang, *Adv. Funct. Mater.* **2011**, *21*, 4519.
[42] X. Fan, X. Li, D. L. Tian, J. Zhai, L. Jiang, *J. Colloid Interf. Sci.* **2012**, *366*, 1.
[43] Y. N. Hong, J. W. Y. Lam, B. Z. Tang, *Chem. Commun.* **2009**, 4332
[44] A. J. Qin, J. W. Y. Lam, B. Z. Tang, *Prog. Polym. Sci.* **2012**, *37*, 182.
[45] L. P. Heng, X. F. Meng, B. Wang, L. Jiang, *Langmuir* **2013**, *29*, 9491.
[46] F. Xia, L. Jiang, *Adv. Mater.* **2008**, *20*, 2842.
[47] F. Mugele, J. C. Baret, *J. Phys.: Condens. Matter* **2005**, *17*, R705.
[48] M. W. J. Prins, W. J. J. Welters, J. W. Weekamp, *Science* **2001**, *291*, 277.
[49] J. P. Youngblood, T. J. McCarthy, *Macromolecules* **1999**, *32*, 6800.
[50] B. Zhao, J. S. Moore, D. J. Beebe, *Science* **2001**, *291*, 1023.